Chemistry Research Journal, 2022, 7(6):1-23

Available online www.chemrj.org

Research Article

ISSN: 2455-8990
CODEN(USA): CRJHA5

Synthesis, Spectral Characterization, Thermal Analysis, Conducting Properties and Biological Activity of Some Cefovecin Metal Complexes

Alaa E. Ali*, Gehan S. Elasala, Tahra Abdelsabour

Chemistry Department, Faculty of Science, Damanhour, Damanhour University, Egypt

Abstract Biologically active [Cr(III), Mn(II), Fe(III), Co(II), Ni(II), Cu(II), Zn(II), Cd(II) and Hg(II)] complexes of cefovecin were prepared and characterized using IR, UV-Vis, ESR, magnetic susceptibility, thermal analysis (TGA and DTA) . IR data pointed that all complexes were suggested that cefovecin coordinates to the metal ions as a bidentate with stochiometries 1:1 (M: L). Electronic absorption spectra gathered with the magnetic moment values proved that all cefovecin complexes have octahedral geometry. The calculated room temperature powdered ESR data of copper cefovecin complex showed anisotropic spectra. Thermal analyses (TGA and DTA) of ligands and their metal complexes were carried out to distinguish between the coordinate and hydrate solvents and to estimate the stability ranges. The thermodynamic parameters, such as activation energy (ΔE*), enthalpy of activation (ΔH*), entropy of activation (ΔS*) and Gibbs free energy (ΔG*) are calculated and discussed. Mössbauer spectroscopy, D.C conductivity measurements and Dielectric constant, A.C. conductivity are discussed. Antimicrobial activities were screened for some metal complexes of cefovecin.

Keywords Coordination chemistry, metal complexes, cefovecin, spectral, thermal analysis, conductivity, Mössbauer spectroscopy, biological activity

Introduction

Cefovecin is a third generation cephalosporin antibiotic has a broad spectrum administered by subcutaneous injection Fig. (1) [1]. It is used to treat skin and soft tissue infections in dogs and cats [2].

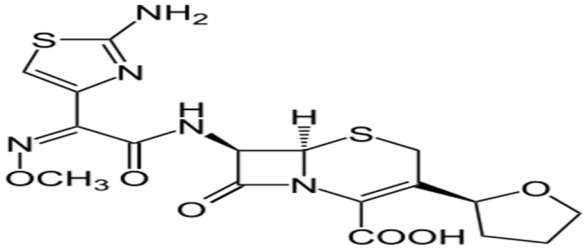

Figure 1: Structure of cefovecin

The antimicrobial effects last for 14 days following administration [3]. In drug studies, cefovecin administered to dogs was 92.4% effective against skin infections (secondary superficial pyoderma, abscesses, and infected wounds). In cats, it was 96.8% effective against skin infections [4]. Ligands play roles in determining the nature e of interactions in target sites, such as DNA, enzymes and protein receptors provide a high diversity for the design of

metallodrugs which may prove a therapeutic activity [5-9]. The aim of the present work is studying the chemical structure, biological activity and thermal behavior of cefovecin and its metal complexes.

Experimental Section

Cefovecin and metal chloride [Cr(III), Mn(II), Fe(III), Co(II), Ni(II), Cu(II), Zn(II), Cd(II) and Hg(II)] were solvated with bidistilled water. The molar amount of the metal chloride salt was reacted with the calculated amount of the ligand with molar ratios (M:L) 1:1. The reaction mixture was refluxed for about 50 min then left overnight, where the formed complexes were filtrated, then washed several times with a mixture of EtOH-H_2O and dried in a vacum desiccator. The analytical results are given in Table 1. The metal contents were analyzed based on atomic absorption technique using model 6650 Shimadzu-atomic absorption spectrophotometer and complexometric titration with standard EDTA solution using the appropriate indicator as reported [10]. The analysis of chloride contents of the complexes were examined by Volhard method [11].

Physical measurements:

1) Metal ion content

The complexes, of accurate weight 0.01-0.02 g, then digested and decomposed by aqua-regia solution. The decomposition step was done several times to ensure that all organic matters were completely destroyed. The residue was dissolved in doubly distilled water. The metal contents were determined based on atomic absorption technique using model 6650 Shimadzu-atomic absorption spectrophotometer and examined complexometrically with standard EDTA solution using the appropriate indicator as reported [10].

2) C, H, N, S and Cl contents

C, H, N and S contents, for all the synthesized complexes, were recorded on CHNS No. 11042023, at central lab, Cairo University. The analysis of chloride contents of the complexes were determined by applying the familiar Volhard method [11].

3) Uv.-Vis. electronic spectra:

The spectrophotometric measurements in ultraviolet and visible spectra regions were recorded by using a double beam spectrophotometer UV-530, Rev. 1.00, PC (JASCO Corp) mode covering the wavelength range 190-900 nm. Two quartz cells of 1 mm thickness were used, one for the test solution and the other for the blank. The spectra of the solid complexes were measured using nujol mull technique [12].

4) Infrared spectra:

The infrared spectra of the ligands and their metal complexes were taken in potassium bromide disc using Perkin Elmer spectrophotometer, Model 1430 covering frequency range of 200-4000 cm^{-1}. Calibration of frequency reading was made with polystyrene film (1602 ± 1 cm^{-1}).

5) Electron spin resonance spectra (ESR):

X-band electron spin resonance spectra were recorded with a reflection spectrometer operating at (9.1-9.8) GHZ in a cylindrical resonance cavity with 100 KHZ modulation. The magnetic field was controlled with a (LMR Gauss meter). The g values were determined by comparison with DPPH signal.

6) Mössbauer spectroscopy

Mössbauer spectroscopy of iron complexes were recorded at room temperature using a computerized Mössbauer spectrometer MS-1200, model: Ranger in standard transmission geometry with a 20 mCi Co^{57}(Rh) source. Mössbauer spectra have been analyzed by means of least square computer fitting using Mössfit computer program. The isomer shift values refer to that of metallic iron at room temperature.

7) Magnetic moment values:

Molar magnetic susceptibilities, corrected for diamagnetism using Pascal,s constants were determined at room temperature (298 °K) using Faraday method. The instrument was calibrated with $Hg[Co(SCN)_4]$ [13].

8) Thermal analysis

Differential thermal analysis (DTA)and thermogravimetric analysis (TGA) of the ligands and their complexes were carried out using a Shimadzu DTA/TGA-50. The rate of heating was 10 °C/min. The cell used was platinum and the

dry nitrogen rate flow over the samples was 10 ml/ min. The chamber cooling water flow rate was 10 l/h. the speed was 5 mm/min. Measurements were achieved by applying the baseline methods. Lipped pans were used to eliminate the sloping of the baseline. A Pt 100 thermocouple was used as temperature sensor.

9) D.C conductivity measurements

The electrical measurements were measured in the temperature range 289–423K. The complexes were prepared in the form of tablets at a pressure of 4 ton cm^{-2}. The tablets were of an area 2.54 cm^2 and thickness 0.12 cm. The samples were hold between two copper electrodes with a silver paste in between and inserted with the holder vertically into cylindrical electric furnace. The potential drop across the heater was varied gradually through VARIAC variable transformer to produce slow rate of increasing temperature to get accurate temperature measurements. The circuit used to measure the electric conductivity consists of D.C. regulated power supply Heat Kit (0–400V), Keith multi-meter for measuring current with a sensitivity up to 10–15A. The temperature of the sample was measured within ±0.1°C by means of copper-constantan T Type thermocouple. This type has excellent repeatability between –380F to 392F (–200ºC to 200ºC). The conductivity was obtained in the case of cooling using the general formula: $\sigma = I \quad d / V_c \quad a$

where '*I*' is the current in ampere, V_c is the potential drop across the sample of cross section area '*a*' and thickness '*d*'.

10) Dielectric constant, A.C. conductivity, study:

The dielectric constant measurements of some selected solid complexes were taken in air on a meter type Hioki 3532 LCR Hitester version 1.02 Japan and cell type (Pw 950/60). Six complexes were pressed into disks of 10 mm diameter and 1-2 mm thickness at a pressure of 9.8 x 10^8 pa. Silver paste was painted on the major faces of each tested piece as electrodes. The measurements of the dielectric constant and the dielectric loss were performed in the frequency range 10^2-10^5 Hz at 25 ºC.

11) Biological activity:

Antimicrobial activity of cefovecin, their metal complexes was determined using the agar well diffusion assay. The tested organisms: *S. pyogenes, K. pneumoniae, P. mirabilis, E. fecalis, S. pneumoniae, P. aeruginosa, E. coli* and *S. aureus* were subcultured on nutrient agar medium (Oxoid laboratories, UK) for bacteria and sabouraud dextrose agar (Oxoid laboratories, UK) and for fungi while antifungal activities were examined against *A. niger, A. flavus, S. racemosum, C. albicans, C. glabrata, F. oxysporum, R. solani* and *A. solani* fungal strains and. The plates were done in triplicate. Bacterial cultures were incubated at 37°C for 24 h, while the other fungal cultures were incubated at (25-30°C) for 3-7 days. Antimicrobial activity was determined by measurement zone of inhibition [14]. The minimum inhibitory concentration (MIC) of the samples was estimated for each of the tested organisms in triplicates. Varying concentrations of the samples (1000-0.007µg/ml), nutrient broth were added and then a loopful of the test organism previously diluted to 0.5 McFarland turbidity standard was introduced to the tubes. A tube containing broth media only was seeded with the test organisms to serve as control. Tubes containing tested organisms cultures were then incubated at 37°C for 24 h, while the other fungal cultures were incubated at (25-30°C) for 3-7 days. The tubes were then examined for growth by observing for turbidity [15].

Table 1: Elemental analysis, melting points and colors of cefovecin (HL^1) complexes.

Complex	Colour	*m.p./^{O}C	Calculated (Found)%					
			C	H	N	S	M	Cl
$[CrL^1Cl_2(H_2O)_2]$	Grey green	240	33.40 (33.39)	3.63 (3.60)	11.45 (11.42)	10.49 (10.46)	8.50 (8.48)	11.60 (11.58)
$[Mn(HL^1)Cl_2(H_2O)_2]$	Buff	200	33.18 (33.20)	3.77 (3.75)	11.38 (11.36)	10.24 (10.25)	8.93 (8.90)	11.52 (11.50)
$[Fe\ L^1Cl_2(H_2O)_2]$	brown	190	33.19 (33.18)	3.60 (3.58)	11.52 (11.48)	10.12 (10.12)	9.08 (9.06)	11.52 (11.49)
$[Co(HL^1)Cl_2(H_2O)_2]$	Pink	290	32.97 (32.96)	3.74 (3.70)	11.45 (11.43)	10.35 (10.34)	9.52 (9.52)	11.44 (11.45)

$[Ni(HL^1)Cl_2(H_2O)_2]$	Pale green	239	32.98 (32.96)	3.74 (3.73)	11.31 (11.30)	10.36 (10.34)	9.48 (9.47)	10.36 (10.35)
$[CuL^1Cl(H_2O)_3]$	Olive green	295	34.52 (34.50)	4.43 (4.41)	11.84 (11.81)	10.84 (10.81)	10.74 (10.72)	5.99 (5.94)
$[ZnL^1Cl(H_2O)_3]$	Off white	232	33.62 (33.60)	3.98 (3.97)	11.53 (11.50)	10.56 (10.53)	10.76 (10.75)	5.84 (5.83)
$[Cd(HL^1)Cl_2(H_2O)_2]$	White	208	30.35 (30.33)	3.45 (3.44)	10.54 (10.53)	9.53 (9.52)	16.71 (16.70)	10.54 (10.52)
$[Hg(HL^1)Cl_2(H_2O)_2]$	Peage	181	26.83 (26.82)	3.05 (3.04)	16.82 (12.80)	8.43 (8.41)	26.36 (26.34)	9.32 (9.30)

*All melting points pointed to starting fusion since the complexes take a range from 4 to 5^{O}C range to be fused completely.

Results and Discussion

All the prepared complexes contain water. In general, water in inorganic salts may be classified as lattice or coordinated water. There is, however, no definite border line between the two. The former term denotes water molecules trapped in the crystalline lattice, either by weak hydrogen bonds to the anion or by weak ionic bonds to the metal, or by both, whereas the latter denotes water molecules bonded to the metal through partially covalent bonds. Although bond distances and angles obtained from X-ray and neutron diffraction data provide direct information concerning the geometry of the water molecule in the crystal lattice. Generally, lattice water absorbs at 3550-3200 cm^{-1} (asymmetric and symmetric OH stretching) [16]. From IR spectra of cefovecin metal complexes, Table (2), one can notice that: The broad band at the range of 3300 – 33500 cm^{-1} in the systems could be assigned to ν_{O-H} involved in hydrogen bond, due to the presence of coordinated water molecules in all prepared complexes while the band at 3310 cm^{-1} could be taken as an indication of lattice water. The stretching vibration bands of C-H located at the range of 2900-3320 cm^{-1}. These bands appeared as weak shoulders due to overlapping with that of the O-H or appeared as normal peak. The coordinated water in these complexes is indicated by the appearance of metal-oxygen bands attributable to rocking modes at 475.99 – 548.22 cm^{-1} region [17]. The lactam (C=O) band appears at 1800 cm^{-1} in the spectrum of cefovecin while the amide (C=O) band appears at 1650 cm^{-1}. The prepared complexes showed the lactam carbonyl band at around 1760-1905 cm^{-1} and show the amide carbonyl band at range 1635-1650 cm^{-1}. All these suggest that coordination of the ligand occurs through the oxygen atom from the lactam carbonyl group rather than the amide carbonyl group. The lactam carbonyl bands were shifted toward higher frequencies relative to the value of the cefovecin while in the amide carbonyl bands, the shifting was not significant. The band at 1399 cm^{-1}, corresponding to the COO asymmetrical stretching of the cefovecin is shifted in the spectra of the complexes, (Cr:1385 cm^{-1}, Mn: 1384 cm^{-1}, Fe: 1327 cm^{-1}, Co: 1345, Ni: 1379 cm^{-1}, Cu: 1345 cm^{-1}, Zn: 1310 cm^{-1}, Cd: 1318 cm^{-1} and Hg: 1340 cm^{-1}), indicating coordination through the C=O of the carboxylate group. Thus, the ligand bound as bidentate ligand forming five membered ring through carboxylic group and N of the lactam ring. The remaining COO bands, ν_{sym}(COO), γ(COO), ω(COO) and ρ(COO) appeared at 1405, 865, 775 and 650 cm^{-1}, respectively, in the cefovecin spectrum . The change in position in the metal complexes spectrum was a result of coordination. The band due to ν_{C-N} of the β-lactam ring (1241 cm^{-1}), is slightly affected by complexation indicating coordination of N-atom β-lactam with the metal ions. This is proved by appearance of ν_{M-N} in the range of 430-440 cm^{-1}. The band of ν_{C-O} of methoxy group (1110 cm^{-1}) and ν_{N-O} of oxime (1045 cm^{-1}) in the cefovecin remain unchanged on complexation. In the far IR spectra, the bonding of oxygen is proved by the presence of bands at 480 – 500 cm^{-1} (M-O)[18]. The metal complexes of cefovecin possess chloride attached to the metal ions which is supported by the presence of υ_{M-Cl}, (less than 400 cm^{-1}) [19]. The bands at range 1000-1100 cm^{-1} were suggested to assign ν_{C-S}.

Table 2: Fundamental infrared bands (cm^{-1}) of cefovecin (HL^1) and its metal complexes

Cefovecin	Cr complex	Mn complex	Fe complex	Co complex	Assignments
3550 (w)	3500 (b)	3495 (b)	3495(b)	3500(b)	ν_{O-H} of H_2O
3300 (w)	3000(w)	2945(w)	2948(w)	2940(w)	ν_{C-H}
1800 (w)	1900(s)	1905(s)	1850(s)	1810(s)	$\nu_{C=O}$ (β- lactam)
1650 (vs)	1639(m)	1649(m)	1642 (s)	1666 (s)	$\nu_{C=O}$ amide
1399 (vs)	1385 (s)	1384 (m)	1327 (m)	1345 (m)	ν_{COO} (asymm)
1405(s)	1405(m)	1403(w)	1406 (m)	1405(m)	ν_{COO} (symm)
1354 (s)	1359 (s)	1350 (w)	1349 (m)	1345(m)	$\nu_{O-CO-CH3}$
1241(s)	1240 (m)	1239 (w)	1236 (s)	1237 (s)	ν_{C-N} (β- lactam)
1110 (w)	1113 (m)	1114 (m)	1115 (w)	1119 (w)	ν_{C-O} of methoxy
1045(vs)	1042 (vs)	1045 (vs)	1041(vs)	1044 (vs)	ν_{N-O} of oxime
865(m)	864(w)	869 (w)	865(w)	863 (w)	γ (COO)
775 (w)	788(w)	774 (w)	775 (w)	776 (w)	ω(COO)
650 (m)	653 (w)	654 (w)	651(w)	650.13(w)	ρ(COO)
------	480 (w)	481(w)	485(w)	481(w)	υ_{M-O}
------	360(w)	369 (w)	375(w)	361 (w)	υ_{M-Cl}
-------	435	437	432	430	υ_{M-N}
1003 (w)	1001 (w)	1005 (w)	1007 (w)	1009	υ_{C-S}

Table (2): Cont.

Ni complex	Cu complex	Zn complex	Cd complex	Hg complex	Assignments
3500(b)	3495(b)	3495(b)	3510(b)	3530(b)	ν_{O-H} of H_2O
2990(w)	2950(w)	2945(w)	3095(w)	3160(w)	ν_{C-H}
1760 (s)	1770(s)	1779(s)	1809 (s)	1871(m)	$\nu_{C=O}$ (β- lactam)
1635(m)	1650 (w)	1648 (s)	1639 (w)	1646 (m)	$\nu_{C=O}$ amide
1379 (m)	1345 (m)	1310 (m)	1318 (m)	1340 (m)	ν_{COO} (asymm)
1405(m)	1407(m)	1409(m)	1406(m)	1408 (m)	ν_{COO} (symm)
1360 (s)	1362 (w)	1367 (w)	1365 (w)	1365 (w)	$\nu_{O-CO-CH3}$
1243 (m)	1243 (s)	1245(m)	1243 (m)	1248(s)	ν_{C-N} (Lactam)
1113 (m)	1114 (w)	1115 (w)	1118 (w)	1120 (w)	ν_{C-O} of methoxy
1045 (vs)	1044(vs)	1043 (vs)	1045 (vs)	1043 (vs)	ν_{N-O} of oxime
865(w)	868 (w)	865 (w)	866(w)	876(w)	γ (COO)
790 (w)	793(w)	689 (w)	693 (w)	699 (w)	ω(COO)
653 (w)	652(w)	650 (w)	655 (w)	659.54(w)	ρ(COO)
480 (w)	485 (w)	481(w)	485 (w)	487(w)	υ_{M-O}
362 (w)	362 (w)	363 (w)	369 (w)	371	υ_{M-Cl}
439	435	432	431	430	υ_{M-N}
1000 (w)	1009 (w)	1015 (w)	1018 (w)	1020	υ_{C-S}

Abbreviations: vs (very strong), s (strong), m (medium), w (weak), b (broad).

Electronic spectra and magnetic susceptibility studies:

The electronic absorption spectra for the Cr^{III}-cefovecin complex, Table (3), showed three bands at 325, 415, 600 nm, respectively due to $^4A_{2g} \rightarrow {}^4T_{2g}$ (F), $^4A_{2g} \rightarrow {}^4T_{1g}$(F) and $^4A_{2g} \rightarrow {}^4T_{1g}$(p) transitions. The complex had a magnetic moment of 3.90 B.M, which is agreed with the value expected for octahedral configurations due to spin only of the complexes. Thus the data indicated that the complex have octahedral geometry in high spin state. The electronic

absorption spectrum of the Mn^{II}- cefovecin complex gave four bands, 310, 359, 440, 525 where the first band is assigned to $^6A_{1g} \rightarrow {}^4A_{1g}$, while the second is due to $^6A_{1g} \rightarrow {}^4T_{2g}$ transition and the last band is due to $^6A_{1g} \rightarrow {}^4T_{1g}$ transition, indicating the Oh geometry [20-21]. Its room temperature μ_{eff} value was 5.80 BM. The low value of magnetism rather than the ideal O_h suggest that there is a type of Mn-Mn interaction with sp^3d^2 hybridization. The structure is based on, bidentate nature of the cefovecin and presence water molecules in the inner sphere.

The electronic absorption spectra of the Fe^{III}-cefovecin complex, showed two bands at 340, 520 nm. The first band is assigned to be CT ($t_{2g} \rightarrow \pi^*$), while the second broad band is due to $^6T_{2g} \rightarrow {}^5E_g$. The CT ($\pi \rightarrow e_g$) band may contribute to the second band resulting in the observed broadening. However, the room temperature magnetic moment value was found to be 5.92 B.M. The data typified the existence of octahedral configuration in high spin state [22-24]. The electronic absorption spectral bands of the Co^{II}-cefovecin complex, gave three bands at 300, 350 and 560 nm. The first two bands are of metal to ligand charge transfer nature and the latter broad bands are assigned to $^4T_{1g}(F) \rightarrow {}^4T_{1g}(P)$ transition typified O_h geometry [25,27]. The band due to $^4T_{1g}(F) \rightarrow {}^4T_{2g}(F)$ transition, which appear usually at 1200 nm is not shown. The magnetic moment value was found to be 3.95 BM, indicated high spin nature of the complex with three unpaired electrons and weak nature of the coordination bonds.

The electronic spectra of the Ni^{II}-cefovecin complex, gave two bands at 345, 558 nm assigned $^3A_{2g}(F) \rightarrow {}^3T_{1g}(P)$ and $^3A_{2g}(F) \rightarrow {}^3T_{1g}(F)$. The broadness is attributed to the existence of more than d-d transition overlapped with each other [25,27]. The room temperature magnetic moment value was 2.8 B.M to assign high spin octahedral configuration. While The electronic spectra of the Cu^{II}- cefovecin complex, gave two bands at 490 and 760 nm. These bands are assumed to be due to $^3B_{1g} \rightarrow {}^2A_{1g}$, and $^2E_g \rightarrow {}^2T_{2g}$ (D), respectively. $^3B_{1g} \rightarrow {}^2T_{2g}$(D) band wasn't appear. The data is assignable to octahedral environment. The room temperature magnetic moment value for Cu^{II}-cefovecin complexes was 1.67 which lower than the value corresponds to one unpaired electron 1.73 B.M due to the probability of the presence of Cu-Cu interaction in the solid state. Zinc, cadmium and mercury complexes of both drug ligands didn't gave visible spectra. All of them were found to be diamagnetic in nature and assumed to be of octahedral geometry like the rest transition metal ions under investigation.

Table 3: Electronic absorption spectra (nm, cm^{-1}) and room temperature magnetic moment values (μ_{eff}, 298°K) B.M of cefovecin complexes

Cefovecin complexes	λ_{max} (nm)	μ_{eff}
Cr^{III} - complex	325, 415, 600	3.90
Mn^{II} - complex	310, 359, 440, 525	5.80
Fe^{III} – complex	340, 520	5.92
Co^{II} - complex	300, 350, 560	3.95
Ni^{II} – complex	345, 558	2.80
Cu^{II} – complex	490, 760	1.67

Electron Spin Resonance of Copper Complex:

The room temperature X-band ESR spectral pattern of Cu-cefovecin complex, Figure (2) and Table (4), represent anisotropic in nature where g// = 2.0263 and $g_{\perp}$= 2.253. The presence of weak signals at g = 4 in complex indicated spin – spin interaction between Cu atoms as a type of Cu-Cu interaction. The <g> values were calculated from the equation: $<g_{//}+2g_{\perp})/3$ to be 2.177. The g values that were found to be more than 2.000 indicated the d_z^2 ground state rather than $d_x^2{}_{-y}^2$. The value of $A_{//}$ = 224 ($\times 10^{-4}$ cm^{-1}) while that $A_{\perp}$= 22.5 ($\times 10^{-4}$ cm^{-1}). These $A_{//}$ values which are more than 100 ($x10^{-4}$ cm^{-1}) prevent the pseudo tetrahedral structure around the copper atoms, indicating the Oh structure of the studied complexes. The G value were 0.01302, i.e. very much less than 4, indicated the presence of very strong interaction between copper atoms in the solid state [28-31]. The data proved the axial compressed nature of cupper complex. Such data are in harmony with previously discussed magnetic properties.

Table 4: Room temperature ESR spectral data for copper (II) complexes

Complex	$g_{\perp}$	$g_{//}$	G	<g>	$A_{//}$	$A_{\perp}$	α^2	f^2
Cu- cefovecin	2.253	2.0263	0.01302	2.177	224	22.5	0.84	0.79

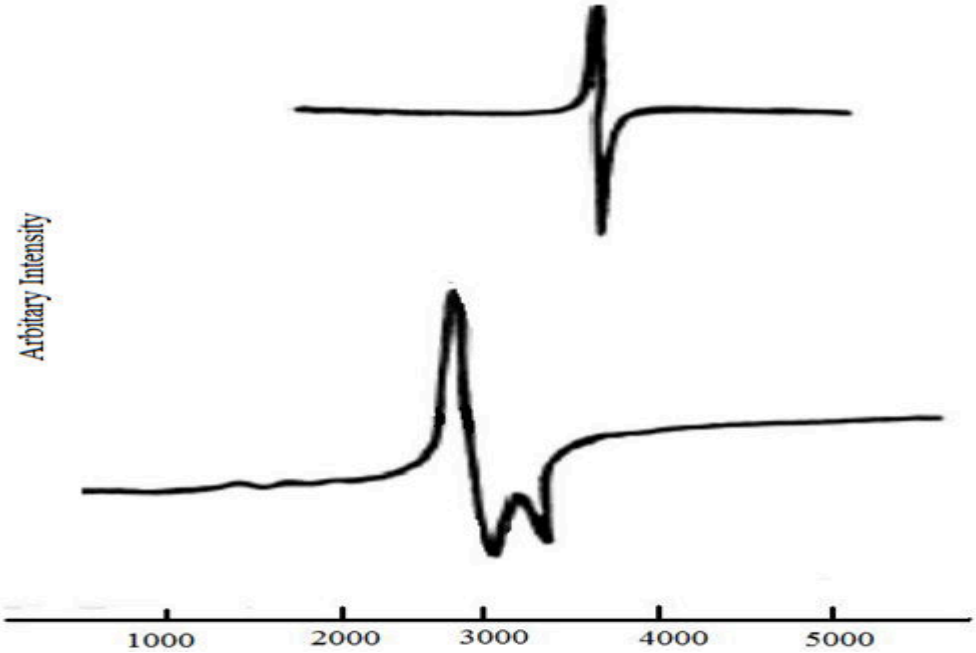

Figure 2: ESR spectrum of Cu-Cefovecin complex

Mössbauer- Spectroscopy

The Mössbauer data of the prepared iron complex of cefovecin displayed a doublet spectral lines each with very close (ΔE_Q = 0.515, δ = O.510, mm/sec.,), Figure (3). Which indicate high spin Fe^{III} complex [32]. The obtained isomer shift values agree with that reported for high spin Fe^{III} complexes (δ~O.5- 0.7mm/sec) [33], and this facilitates the geometry that supposed and the values of μ_{eff} obtained before for the two complexes.

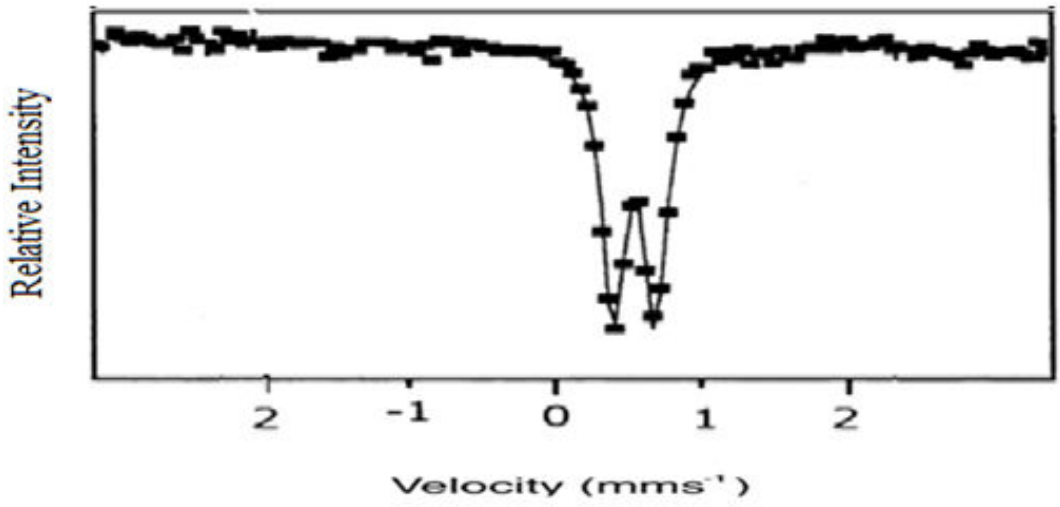

Figure 3: Mössbauer- Spectroscopy of Fe^{III}- cefovecin complex

From the IR data gathered with the electronic spectra, magnetic susceptibility measurements, ESR spectra and *Mössbauer Spectroscopy*, the structures of the prepared complexes collected in Figure (4).

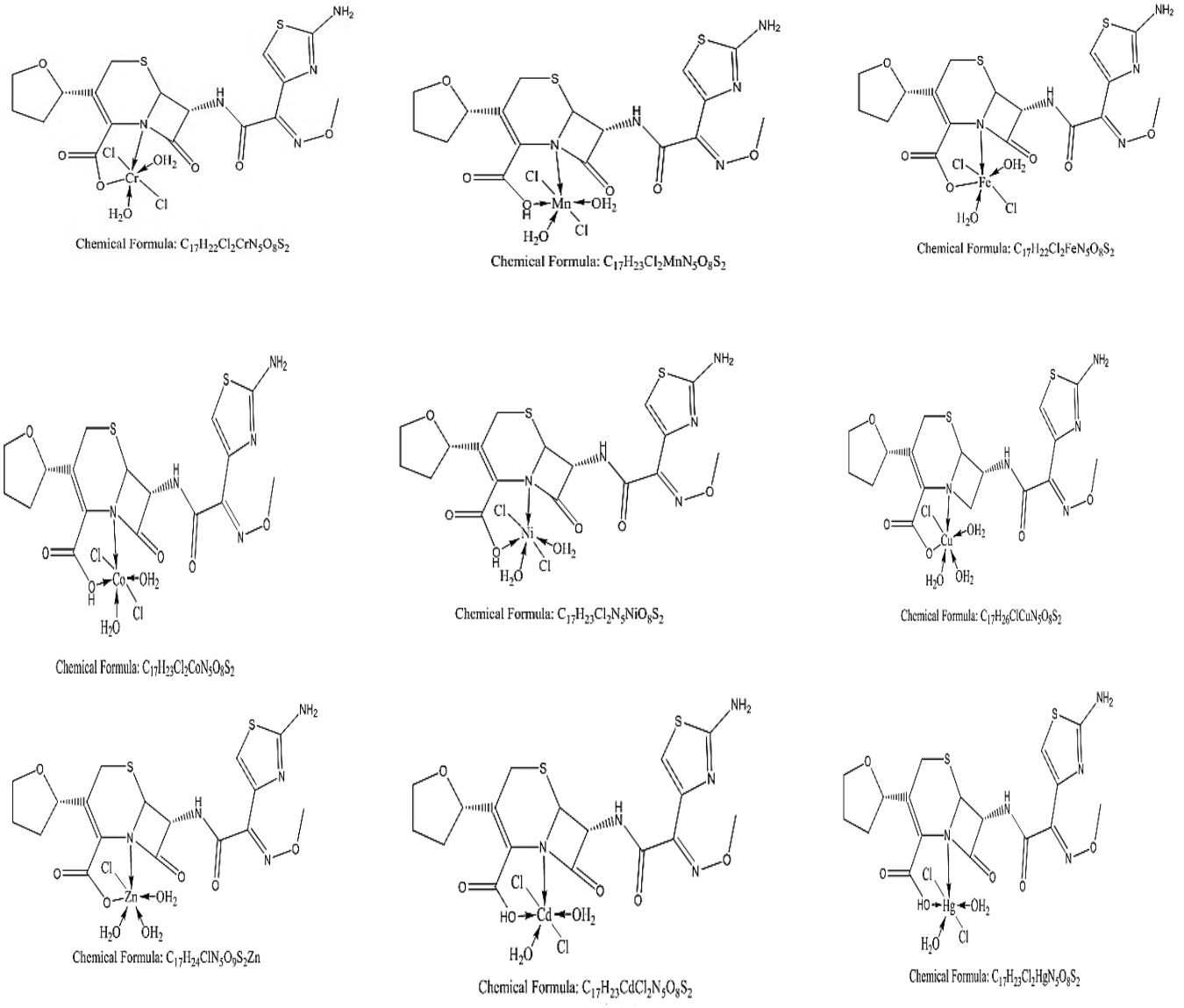

Figure 4: Proposed structures of Cefovecin complexes

Thermal analysis

The thermal behavior of cefovecin and some metal complexes were investigated by thermograms TG and DTA curves, Figure (6) of cefovecin, gave five peaks. The 1st was endothermic and the rest were exothermic. The orders of the corresponding thermal dissociation steps were 1.26, 1.23, 2.33 0.97 and 1.03 respectively, with activation energies of 33.24, 18.78, 47.75, 23.75, and 70.56 kJ/mol, respectively. The dissociation steps left no residue. ΔS values for the five steps ranged from -0.12 to -0.13 kJ/mol, Table (5), indicating that the transition states of the dissociation steps were more ordered than reactants and all steps proceeded by same trend. ΔH and collision number Z values for the dissociation steps are given in Table (5). The mechanism of the dissociation, Figure (5), is suggested to be removal of 2-amino- 1,3-thiazol, step I then the methoxyiminoacetyl amino with decarboxylation, step II then oxolan, step III then thia- 1-azabicyclo[4.2.0]oct- 2-ene in two steps, IV and V.

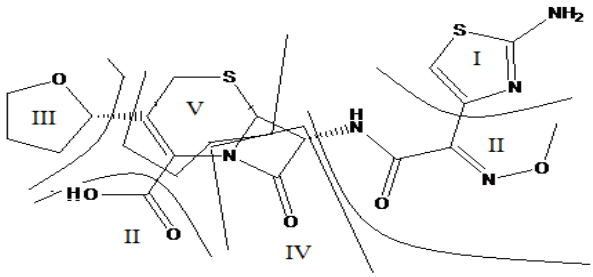

Figure 5: The steps, I-V of the thermal dissociation of cefovecin

The TG and DTA curves of Cr-cefovecin complex, gave two peaks. The 1st was endothermic and the 2nd was exothermic. The orders of the corresponding thermal dissociation steps were 2.16 and 1.45 respectively, with activation energies of 39.07 and 30.11 kJ/mol respectively. The dissociation steps left Cr_2O_3 as final product. ΔS values for the two steps ranged were -0.12 and -0.13 kJ/mol, Table (5), indicating that the transition states of the dissociation steps were more ordered than reactants and the steps proceeded by same trend. ΔH and collision number Z values for the dissociation steps are given in Table (5). The mechanism of the dissociation is suggested to be like that of cefovecin itself but only in two steps to form Cr(III) oxide.

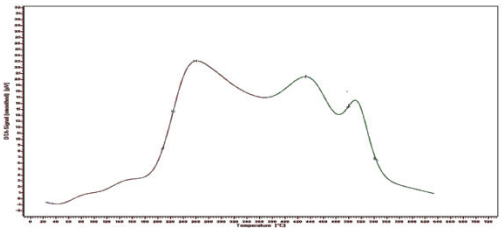

DTA of Cefovecin

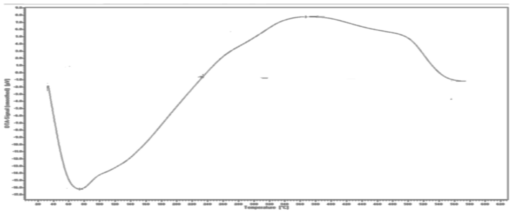

DTA of Cr-Cefovecin

Figure 6: DTA of studied Cefovecin and its Cr-complex as an example

Table 5: Kinetic parameters of dissociation steps for cefovecin and its metal complexes

Cefovecin							
T	**n**	**β**	**α**	**Ea(kJ/mol)**	**ΔH(kJ/mol)**	**Z S^{-1}**	**ΔS (kJ/mol)**
46.00	1.26	2.41	0.59	33.24	-38.59	31.41	-0.12
161.00	1.23	2.38	0.59	18.78	-54.70	12.54	-0.13
261.00	2.33	3.14	0.47	47.75	-61.89	34.46	-0.12
432.00	0.97	1.94	0.63	23.75	-88.71	7.91	-0.13
512.00	1.03	2.06	0.63	70.56	-91.23	22.58	-0.12
Cr							
74.00	2.16	3.08	0.49	39.07	-40.80	43.37	-0.12
360.00	1.45	2.63	0.56	30.11	-76.79	15.18	-0.12
Mn							
100.00	1.54	2.70	0.55	25.20	-45.68	22.42	-0.12
460.00	0.87	1.71	0.66	18.59	-94.51	5.24	-0.13
Fe							
76.00	1.68	2.81	0.53	51.08	-40.49	52.02	-0.12
235.00	1.46	2.63	0.56	61.11	-58.55	39.15	-0.12
320.00	0.98	1.96	0.64	16.53	-76.36	6.61	-0.13
570.00	0.75	1.34	0.68	129.38	-96.68	25.28	-0.11
Co							
86.00	1.87	2.93	0.51	46.23	-41.84	47.38	-0.12
243.00	1.37	2.54	0.57	130.75	-56.23	82.12	-0.11

307.00	1.41	2.58	0.57	165.48	-61.99	93.93	-0.11
400.00	1.23	2.37	0.59	64.71	-77.89	27.88	-0.12
516.00	0.72	1.22	0.69	42.94	-98.42	8.05	-0.12
580.00	1.08	2.15	0.62	311.12	-88.04	99.29	-0.10
Ni							
93.00	1.71	2.83	0.53	31.80	-43.95	30.43	-0.12
245.00	1.07	2.14	0.62	86.74	-59.04	44.81	-0.11
535.00	0.58	0.53	0.73	11.10	-115.53	0.88	-0.14
Cu							
74.00	1.95	2.98	0.50	31.70	-41.52	33.79	-0.12
240.00	1.40	2.57	0.57	62.29	-59.14	38.62	-0.12
340.00	1.13	2.24	0.60	30.73	-75.07	13.64	-0.12
550.00	0.68	1.07	0.70	47.63	-102.85	7.51	-0.12
Zn							
90.00	1.83	2.90	0.51	34.41	-43.27	34.12	-0.12
252.00	1.50	2.67	0.56	119.59	-57.41	77.07	-0.11
346.00	1.20	2.33	0.60	18.24	-78.31	8.30	-0.13
563.00	0.55	0.39	0.73	58.43	-110.06	3.31	-0.13
Cd							
95.00	1.92	2.96	0.51	28.67	-44.38	28.45	-0.12
259.00	1.21	2.35	0.60	117.49	-58.83	65.62	-0.11
403.00	1.32	2.49	0.58	27.96	-82.73	12.48	-0.12
566.00	1.07	2.14	0.62	125.76	-93.15	39.42	-0.11
Hg							
104.00	2.39	3.16	0.47	17.00	-46.93	17.38	-0.12
342.00	1.32	2.48	0.58	414.03	-60.87	229.06	-0.10
451.00	1.29	2.45	0.58	179.04	-77.33	75.92	-0.11

Electrical conductivity measurements

The electrical conductivity data are represented in Figures (7-10) and collected in Tables (6-7). The data depict that all complexes are of semiconductor behaviour. The discontinuation in the conductivity curves of the complexes can be argued to be a molecular rearrangement. This is a character taking place in some complexes with semi conducting behavior. Semiconductor material at 0 K has the same properties of insulators. For an example the conductivity of Cr-cefovecin complexes showed three regions with temperature breaks at 40 and 120 ^{o}C, Figures (7-8). The ΔEa - $ln\sigma_o$ curve, Figure (11), gave the following equation for the conduction of chromium cefovecin complex:

$$\Delta Ea = 3x10^{-5} \ln \sigma_o + 0.0005$$

The temperature dependence of the conductivity curves of the manganese cefovecin complex, Figures (9-10), showed that conductivity increases with temperature. The conductivity pattern of Mn-cefovecin complex, exhibits three regions with transition temperature of 35 and 160°C. The breaks agree with the TG pattern leading a good agreement with the thermal analysis data. The ΔEa - $ln\sigma_o$ curve, Figure (12), gave the following empirical equation for the conduction of manganese cefovecin complex:

$$\Delta Ea = 62.506 \ln \sigma_o - 0.0287$$

Generally, this data proved the semiconducting behavior of these metal cefpodoximee complexes. The $\ln \sigma_o$ and ΔEa values of this complexes are collected in Table (8). Similar empirical equation for the conduction of other metals complex with cefovecin

Fe-cefovecin complex	$\Delta Ea = 1x10^{-05} \ln \sigma_o + 0.0003$
Co-cefovecin complex	$\Delta Ea = 3x10^{-05} \ln \sigma_o + 0.0005$
nickel cefovecin complex	$\Delta Ea = 0.5557 \ln \sigma_o + 0.0001$
Cu-cefovecin complex	$\Delta Ea = 0.5692 \ln \sigma_o + 0.0002$
zinc cefovecin complex	$\Delta Ea = 0.0158 \ln \sigma_o + 0.0006$
Cd-cefovecin complex	$\Delta Ea = 4.30163x10^{5} \ln \sigma_o.$
mecury cefovecin complex	$\Delta Ea = 0.6687 \ln \sigma_o + 0.0001$

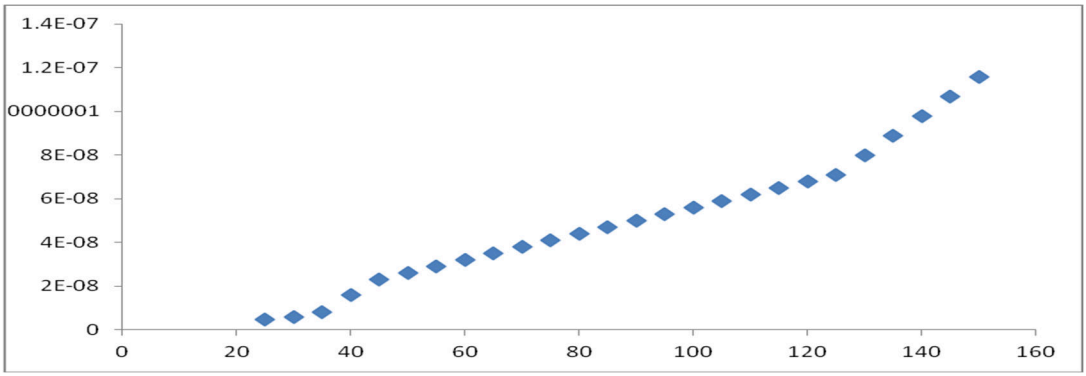

Figure 7: σ relation with T/°C for Cr-cefovecine complex

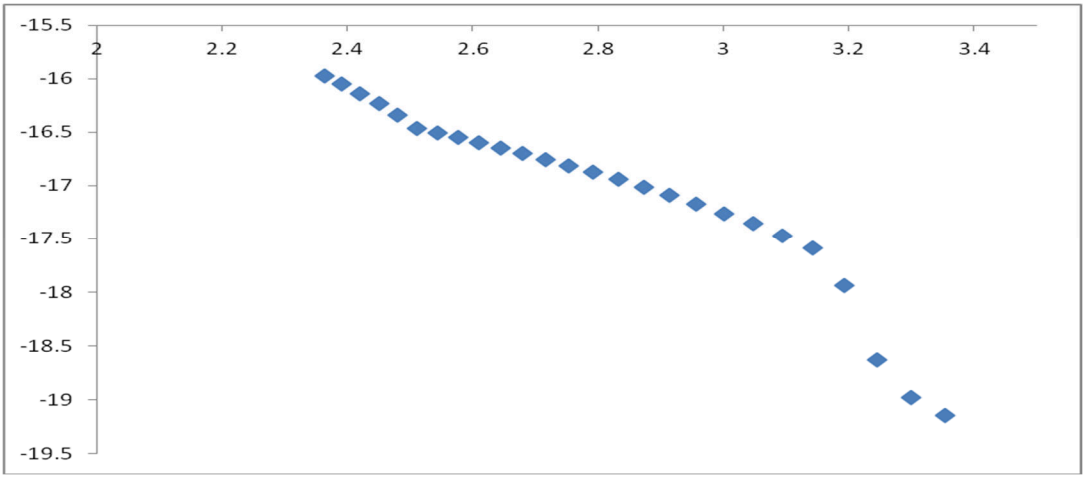

Figure 8: Ln σ relation with 1000/T/ for Cr-cefovecine complex

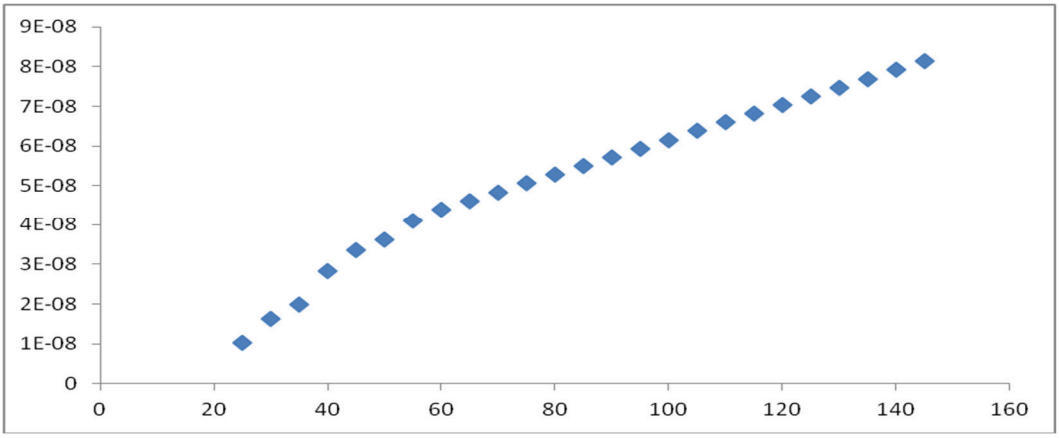

Figure 9: σ relation with T/°C for Mn-cefovecine complex

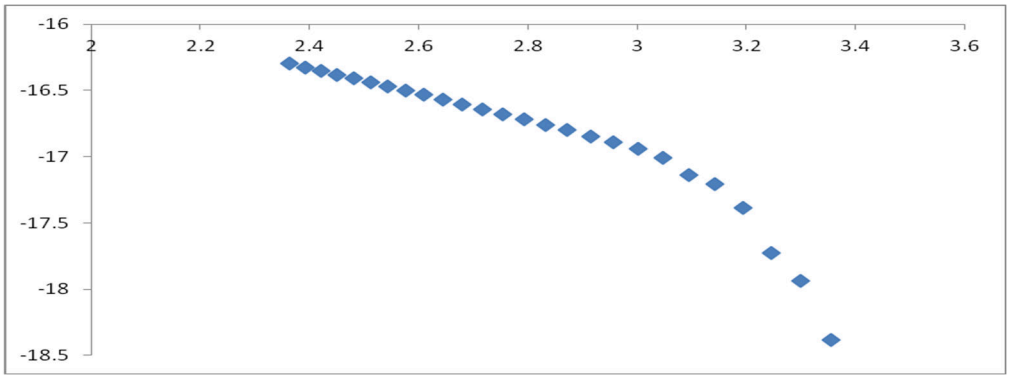

Figure 10: Ln σ relation with 1000/T/ for Mn-cefovecine complex

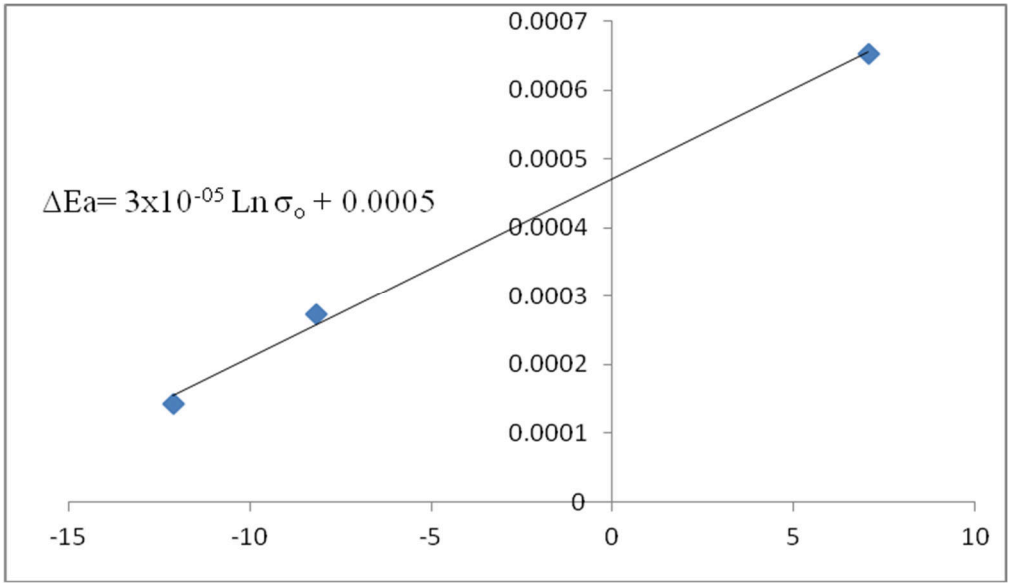

Figure 11: ΔE_a- Ln σ_o for Cr - cefovecin complex

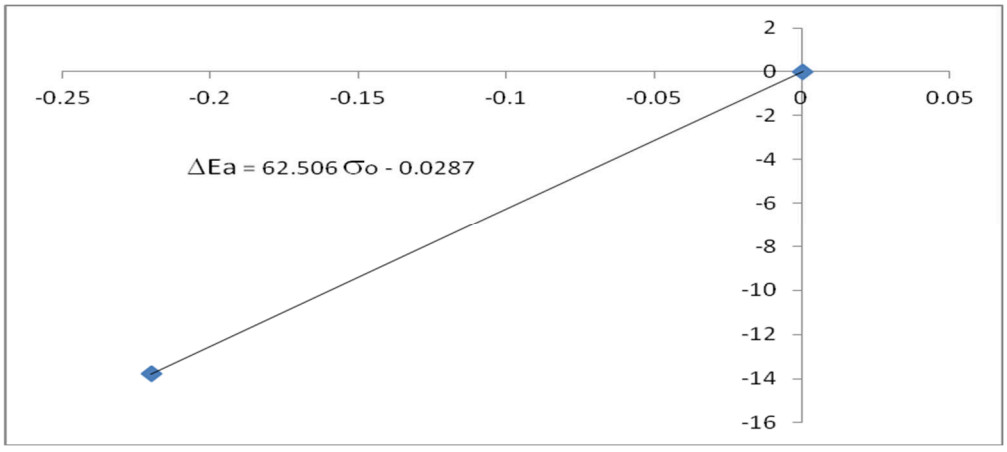

Figure 12: ΔE_α- Ln σ_o for Mn - cefovecin complex

Table 6: The values of conductivity at different temperature for Cr cefovecin complex

T/^{O}C	σ /ohm^{-1} cm^{-1}	T/ K	Ln σ
25	4.8246X10^{-09}	3.35401641	-19.1495
30	5.72922X10^{-09}	3.298697029	-18.9777
35	8.0883X10^{-09}	3.24517282	-18.6328
40	1.61766X10^{-08}	3.193357767	-17.9397
45	2.2917X10^{-08}	3.143171454	-17.5914
50	2.5917X10^{-08}	3.09453814	-17.4684
55	2.8917X10^{-08}	3.047386866	-17.3588
60	3.1917X10^{-08}	3.001650908	-17.2601
65	3.4917X10^{-08}	2.957267501	-17.1703
70	3.7917X10^{-08}	2.914177473	-17.0879
75	4.0917X10^{-08}	2.872325129	-17.0117
80	4.3917X10^{-08}	2.831657964	-16.941
85	4.6917X10^{-08}	2.792126214	-16.8749
90	4.9917X10^{-08}	2.753683043	-16.8129
95	5.2917X10^{-08}	2.716284126	-16.7545
100	5.5917X10^{-08}	2.679887453	-16.6994
105	5.8917X10^{-08}	2.644453259	-16.6471
110	6.1917X10^{-08}	2.609943886	-16.5975
115	6.4917X10^{-08}	2.576323586	-16.5502
120	6.7917X10^{-08}	2.543558438	-16.505
125	7.0917X10^{-08}	2.511616225	-16.4618
130	7.9917X10^{-08}	2.480466328	-16.3423
135	8.8917X10^{-08}	2.450079628	-16.2356
140	9.7917X10^{-08}	2.420428416	-16.1391
145	1.06917X10^{-07}	2.391486309	-16.0512
150	1.15917X10^{-07}	2.36322817	-15.9704

Table 7: The values of conductivity at different temperature for Mn cefovecin complex

T/^{O}C	σ /ohm^{-1} cm^{-1}	T/ K	Ln σ
25	1.03766X10^{-08}	3.35401641	-18.3837
30	1.61766X10^{-08}	3.298697029	-17.9397
35	1.99739X10^{-08}	3.24517282	-17.7288
40	2.81952X10^{-08}	3.193357767	-17.3841
45	3.36515X10^{-08}	3.143171454	-17.2072
50	3.61078X10^{-08}	3.09453814	-17.1368
55	4.09267X10^{-08}	3.047386866	-17.0115
60	4.39219X10^{-08}	3.001650908	-16.9409
65	4.61231X10^{-08}	2.957267501	-16.892
70	4.83242X10^{-08}	2.914177473	-16.8453
75	5.05254X10^{-08}	2.872325129	-16.8008
80	5.27265X10^{-08}	2.831657964	-16.7581
85	5.49277X10^{-08}	2.792126214	-16.7172
90	5.71289X10^{-08}	2.753683043	-16.678
95	5.933X10^{-08}	2.716284126	-16.6402
100	6.15312X10^{-08}	2.679887453	-16.6037
105	6.37323X10-08	2.644453259	-16.5686
110	6.59335X10^{-08}	2.609943886	-16.5346
115	6.81346X10^{-08}	2.576323586	-16.5018

120	$7.03358X10^{-08}$	2.543558438	-16.47
125	$7.25369X10^{-08}$	2.511616225	-16.4392
130	$7.47381X10^{-08}$	2.480466328	-16.4093
135	$7.69392X10^{-08}$	2.450079628	-16.3802
140	$7.91404X10^{-08}$	2.420428416	-16.352
145	$8.13416X10^{-08}$	2.391486309	-16.3246
150	$8.35427X10^{-08}$	2.36322817	-16.2979

Table 8: Ln σ_o and ΔEa for cefovecin complexes

Slope of Ln σ_o – 1000/T relation	**Ln σ_o**	**ΔEa / eV**
Cr – complex		
-3.3	-8.15	0.000274379
-1.72	-12.1	0.00014301
-7.85	7.05	0.000652689
Mn – complex		
-5.53	0.22	0.000459792
-1.06	-13.78	$8.81338x10^{-05}$
Fe – complex		
-0.35	-17.23	$2.91008 x10^{-05}$
-2.59	-9.72	0.000215346
-3.67	7.2	0.000305143
Co – complex		
-0.35	-17.23	$2.91008 x10^{-05}$
-2.68	-9.46	0.000222829
-3.43	-7.77	0.000285188
Ni – complex		
-0.48	-16.75	$3.99096 x10^{-05}$
-2.09	-11.15	0.000173773
Cu		
-0.17	-17.78	$1.41347 x10^{-05}$
-2.53	-10.12	0.000210357
Zn – complex		
-1.3	-13.94	0.000108089
-7.03	0.22	0.00058451
Cd – complex		
-0.47	-16.81	$3.90782 x10^{-05}$
Hg – complex		
-0.48	-16.75	$3.99096 x10^{-05}$
-2.07	-11.2	0.00017211

Dielectric Studies

The mode of this descriptive studies is based on changing the frequency from 0.1 to 100 kHz and recording the potential difference, V, the phase angle, θ, the dielectric loss, D and the capacitance, C, at 30 °C. The relation between frequency and potential is shown in Figures (13) for studied cefovecin metal complexes. In case of Cefovecin complexes, Zn and Cd complexes gave same trend and this may be due to the nature of the ligand, so we can say that there is a remarkable change may be attributed to the nature of the ligand.

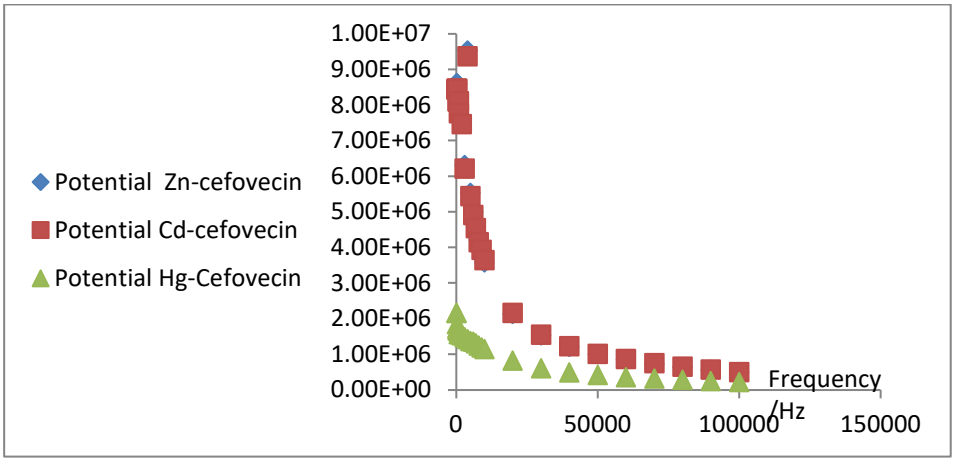

Figure 13: Potential – Frequency relation for cefovecin complexes

The capacity – frequency relationships for cefovecin complexes were shown in Figures (14), the capacity values decrease then reach stable values. The Zn and Cd cefovecin complexes gave same and this agree with the potential – frequency relationships.

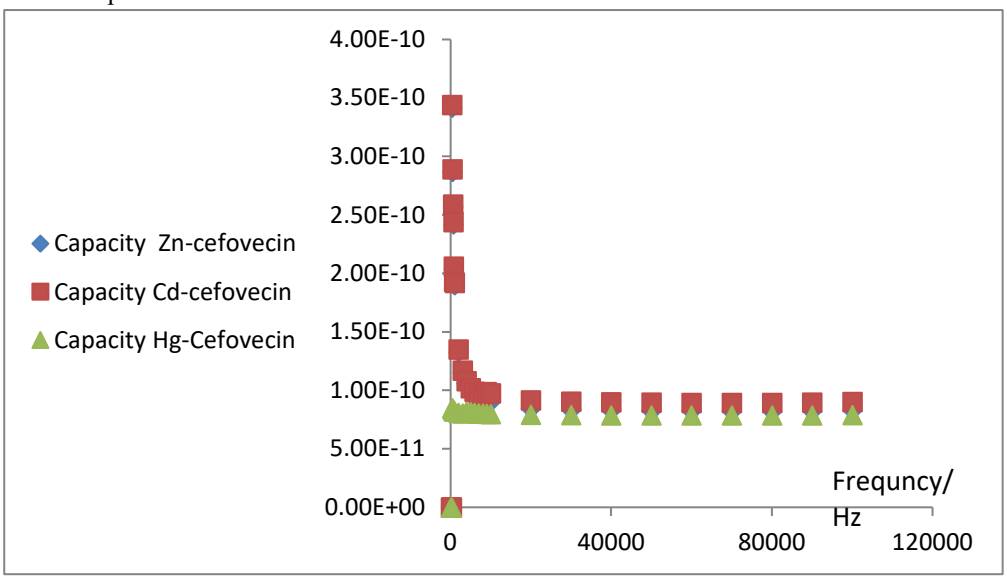

Figure 14: Capacity – Frequency relation for cefovecin complexes

The mode of this descriptive studies is based on changing the frequency from 0.1 to 100 kHz and recording the potential difference, V, the phase angle, θ, the dielectric loss, D and the capacitance, C, at 30 °C. The relation between frequency and potential is shown in Figures (15) for studied cefovecin complexes. In case of Cefovecin complexes, Zn and Cd complexes gave same trend this may be due to the nature of the ligand, so we can say that there is a remarkable change may be attributed to the nature of the ligand.

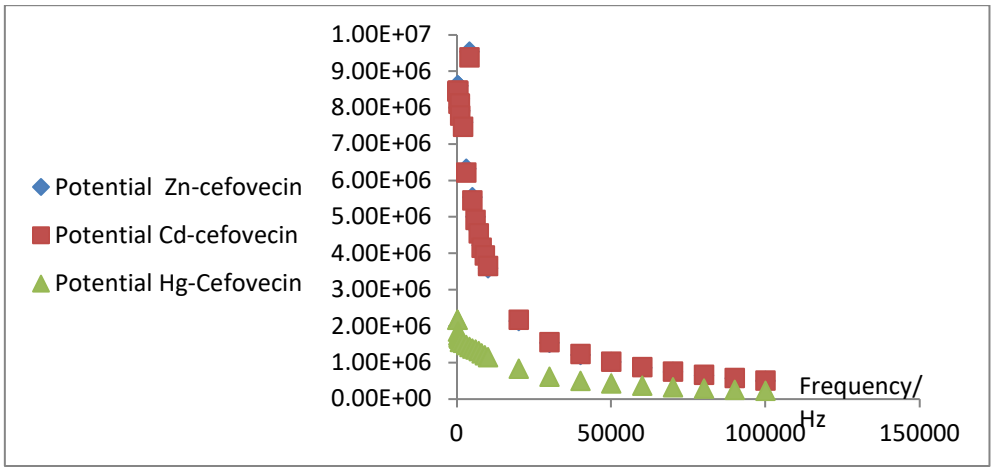

Figure 15: Potential – Frequency relation for cefovecin complexes

The capacity – frequency relationships for cefovecin complexes were shown in Figure (16). The capacity values decrease then reach stable values. The Zn and Cd cefovecin complexes gave same trend and this agree with the potential – frequency relationships.

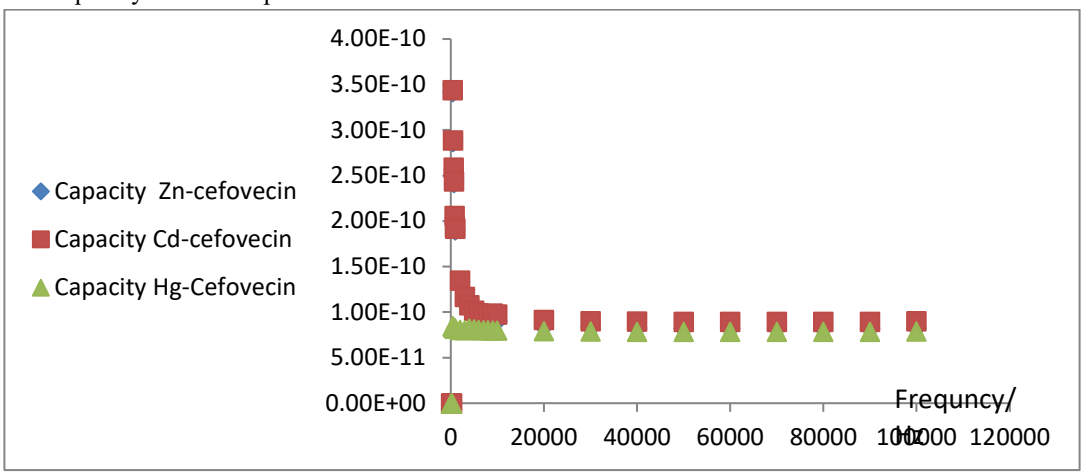

Figure 16: Capacity – Frequency relation for cefovecin complexes

For the dependence of the dielectric loss, D, on frequency, Figures (17), it is found that the D values for both of Zn and Cd cefovecin complexes starts to increase at law values of frequencies then the change will be very small at high frequencies within narrow range of D values. In case of Hg cefovecin complex, the D values at law frequencies are relatively high then decrease to the same narrow range of both Zn and Cd complex

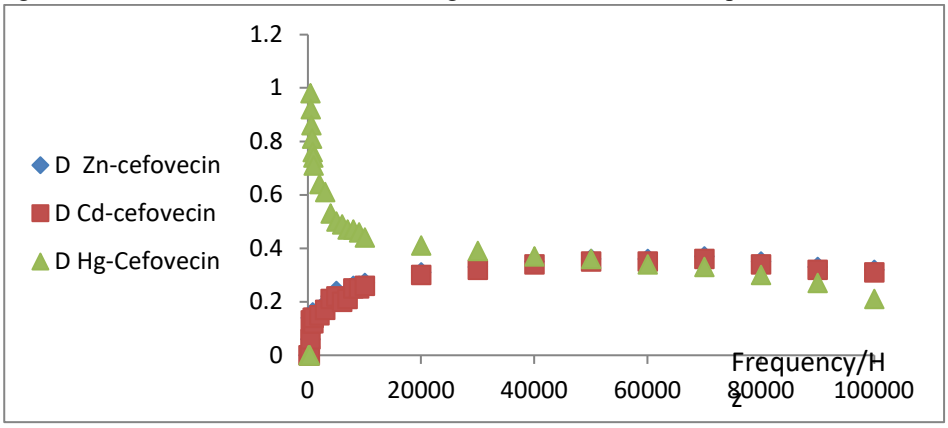

Figure 17: Dielectric Loss – Frequency relation for cefovecin complexes

It is known that the permittivity value, ε, depends on the changeable external factors (the frequency of the voltage applied to the dielectric and the temperature). Also, it was reported that the permittivity of non-polar dielectrics does not depend on frequency when it changes within the very broad limits and for cases of dipole polarization, when the frequency of alternating voltage increases, the value of ε for a polar dielectric at first remains invariable then begins to decrease by increasing the frequency [34,35]. In our study the ε values decrease for all complexes with increasing frequency values till reach very law values, near zero, at high frequency, Figures (18), i.e. at high frequencies, ε values reach the values of typical non-polar dielectrics and this is recorded in cefovecin complexes.

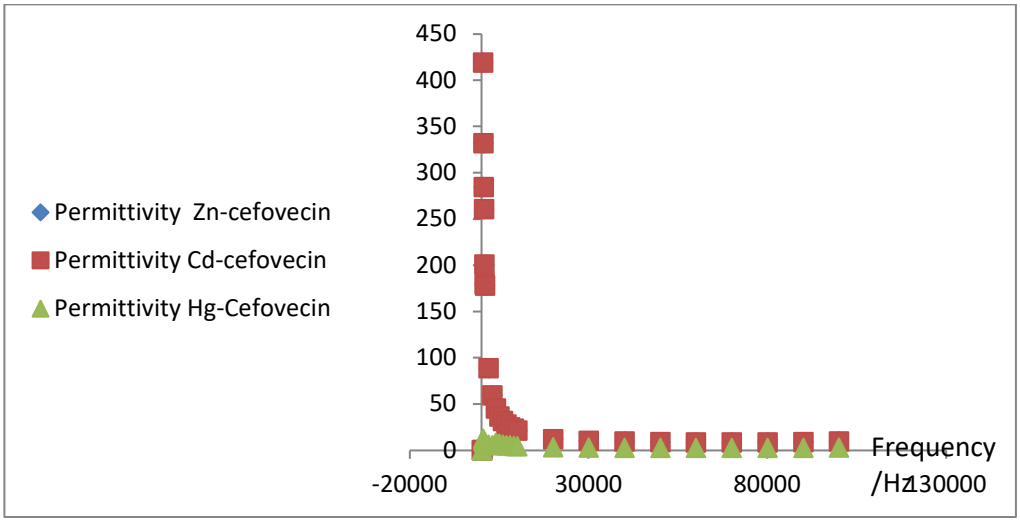

Figure 18: Permittivity – Frequency relation for cefovecin complexes

The conductivity dependence on frequency is shown in Figure (19). In case of cefovecin complexes, the conductivity values of Hg complex are higher than that of both Zn and Cd complex. One can arrange conductivity values as follows: Hg > Cd ≈ Zn complex for cefovecin complexes.

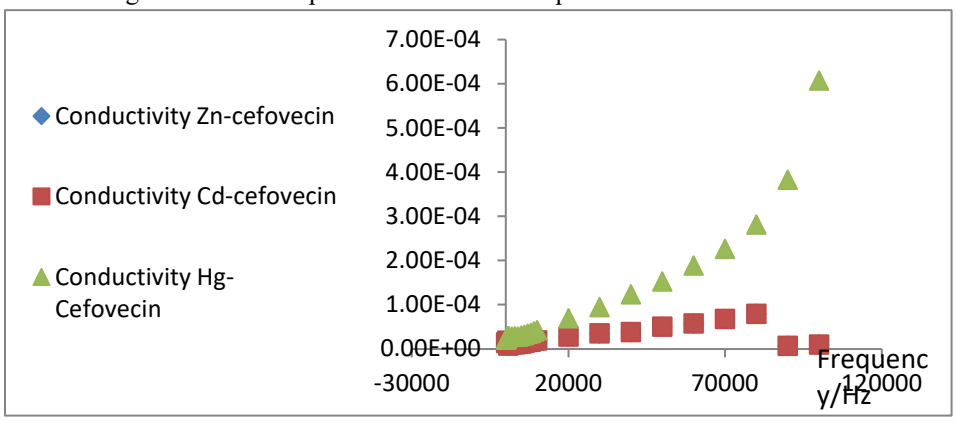

Figure 19: Conductivity – Frequency relation for cefovecin complexes

Antibacterial activity:

The *in vitro* antimicrobial screening of cefovecine, and their complexes were performed against the following bacterial strains, *S. pyogenes*, *K. pneumoniae*, *P. mirabilis*, *E. fecalis*, *S. pneumoniae*, *P. aeruginosa*, *E. coli* and *S. aureus* and their efficiency against the bacteria was compared with the free ligands, Table (9) and Figures (20-21). The minimum inhibitory concentration (MIC) of some selected complexes, which showed significant activity against the selected bacterial species, was determined in comparison to the standard antibiotic cefovecin are clooecte in Table (10). The values indicate that the complexes are potentially good inhibitors of the bacterial organisms. The

values for the complexes were found to be slightly more or less than that of free antibiotic. For cefovecin the values of inhibitions were ranged from 14.3 to 21.7 for *P. aeruginosa* and *S. pyogenes*, respectively. This is the case for Zn-cefovecin complex. These values changed in Cr-cefovecin complex to the range of 15.4-20.3 and Cd-cefovecin range of 14 to 19.4 for *E. fecalis* and *S. aureus,* respectivly while for *Mn*-cefovecin *and* Co-cefovecine complexes the range is 11.7 *to* 15.2 and is 13.3 to 15.2 for *K. pneumoniae* and *E. coli, respectively.* In case of Fe-cefovecine the range exceeds therange of cefovecine, 14.3 to 22.4 for *P. aeruginosa* and *S. pyogenes*, respectively this is repeated in case of Cu-cefovecin complex, 14.3 to 24.7 and in case of Hg-cefovecin complex, 14.3 to 23.4 for *P. aeruginosa* and *S. pyogenes*, respectively. The minimum and the maximum value of Ni-cefovecin complex were 17.4 and 22 for *P. aeruginosa* and *E. coli*. The MIC values for antibacterial activity are shown in Table (11).

Antifungal activity

Antifungal activity of cefovecin, and their metal complexes were examined against *A. niger*, *A. flavus*, *S. racemosum*, *C. albicans*, *C. glabrata*, *F. oxysporum*, *R. solani* and *A. solani* fungal strains and illustrated in Table (12) and Figures (20-21). The minimum inhibitory concentration (MIC) of the selected complexes was determinedand summarized in Table (9). The values indicate that the complexes are potentially good inhibitors of the fungi organisms. By the same mode of discussion, it is found that the minimum values of inhibition were recorded for cefovecin, and most of their complexes for the fungi named *R. solani,* while the maximum values were recorded to *F. oxysporum,* Table (12).

Table 9: Antibacterial activity of cefovecin, and their metal complexes

Compounds	***S.pyogenes* (RCMB010015)**	***K.pneumoniae* (RCMB001009)**	***P.mirabilis* (RCMB010085)**	***E.fecalis* (RCMB010075)**	***S.pneumoniae* (RCMB010029)**	***P.aeruginosa* (RCMB010043)**	***E.coli* (RCMB010056)**	***S.aureus* (RCMB010027)**
Cefovecin	21.7	15.1	14.9	18.6	19.1	14.3	16.7	19.7
Cr – cefovecin complex	19.3	19.7	16.3	15.4	19	14.3	19	20.3
Mn- cefovecin complex	12.7	11.7	14.9	14.8	12.8	14.3	15.2	14
Fe- cefovecin complex	22.4	21.4	18.9	17.4	20.6	14.3	22.2	21.3
Co- cefovecin complex	14.7	13.3	14.9	14.8	13.9	14.3	15.2	15.3
Ni- cefovecin complex	21.4	20	17.5	18.6	21.6	17.4	22	20.8
Cu- cefovecin complex	24.7	17.2	17.7	23.8	22.6	14.3	19	22.5
Zn- cefovecin complex	21.7	20.2	17.7	16.2	19.2	14.3	20.7	20.8
Cd- cefovecin complex	18.9	18.8	14.7	14	18.5	14.3	19.2	19.4
Hg- cefovecin complex	23.4	21.79	18.4	17.3	20.6	14.3	21.2	22.3

Table 10: MIC (μg/ml) for antibacterial activity of cefovecin, and their metal complexes

Compounds	***S.pyogenes* (RCMB010015)**	***K.pneumoniae* (RCMB001009)**	***P.mirabilis* (RCMB010085)**	***E.fecalis* (RCMB010075)**	***S.pneumoniae* (RCMB010029)**	***P.aeruginosa* (RCMB010043)**	***E.coli* (RCMB010056)**	***S.aureus* (RCMB010027)**
Cefovecin	1.15	52.50	44.50	7.21	1.70	3.60	30.25	2.70
Cr – cefovecin complex	7.01	1.95	10.23	30.65	8.25	3.60	0.95	0.33
Mn- cefovecin complex	41.20	44.50	1.05	3.20	22.80	3.60	2.80	13.40
Fe- cefovecin complex	0.18	0.65	0.55	7.21	4.02	3.60	0.24	0.49
Co- cefovecin complex	24.20	17.00	1.05	3.20	60.30	3.60	2.80	30.05
Ni- cefovecin complex	0.11	4.65	1.15	3.30	0.04	3.60	0.12	1.41
Cu- cefovecin complex	0.04	5.60	10.23	9.48	0.04	3.70	6.81	0.33
Zn- cefovecin complex	0.18	1.15	1.15	15.03	1.75	3.60	0.43	0.33
Cd- cefovecin complex	0.18	2.75	25.85	0.94	0.29	3.60	14.63	0.33
Hg- cefovecin complex	0.23	0.10	0.55	1.35	1.02	1.75	0.06	0.12

Table 11: Antifungal activity of cefovecin, and their metal complexes

Compounds	***A.niger* (RCMB2317)**	***A.flavus* (RCMB02426)**	***S.racemosum* (RCMB05922)**	***C.albicans* (RCMB05031)**	***C.glabrata* (RCMB05274)**	***F.oxysporum* (RCMB08213)**	***R.solani* (RCMB09421)**	***A.solani* (RCMB07324)**
-Amphotericin B standard	20.4	17.3	20.7	22.0	21.7	24.6	26.7	24.3
Cefovecin	11.20	5.70	4.20	2.00	10.30	12.10	1.00	8.80
Cr – cefovecin complex	17.90	19.90	15.30	1.50	15.20	20.90	0.90	12.95
Mn- cefovecin complex	13.20	6.00	13.35	2.20	11.30	16.20	1.40	9.80
Fe- cefovecin complex	18.90	19.95	17.50	2.30	15.40	21.30	1.80	13.70
Co- cefovecin complex	11.90	4.30	10.45	1.60	10.50	12.30	1.05	9.70
Ni- cefovecin complex	18.15	19.25	17.75	1.20	16.20	20.80	1.47	12.55
Cu- cefovecin complex	16.75	12.20	15.60	1.10	15.30	22.20	0.88	1.85
Zn- cefovecin complex	12.90	12.35	13.55	1.60	13.60	14.90	1.25	9.95
Cd- cefovecin complex	15.20	16.85	14.50	2.80	13.80	21.20	0.72	2.45
Hg- cefovecin complex	14.25	12.60	14.90	1.25	13.90	15.50	1.27	2.50

Table 2: MIC for antifungal activity of cefovecin and their metal complexes

Compounds	*A.niger* (RCMB2317)	*A.flavus* (RCMB02426)	*S.racemosum* (RCMB05922)	*C.albicans* (RCMB05031)	*C.glabrata* (RCMB05274)	*F.oxysporum* (RCMB08213)	*R.solani* (RCMB09421)	*A.solani* (RCMB07324)
Amphotericin B Standard	0.49	3.9	0.49	0.12	0.24	0.03	0.007	0.03
Cefovecin	124.60	170.00	53.50	1.20	248.90	249.90	0.80	300.40
Cr – cefovecin complex	3.50	0.98	2.30	1.30	6.70	0.14	0.95	62.45
Mn- cefovecin complex	7.40	3.05	7.75	2.00	2.80	7.70	0.70	61.90
Fe- cefovecin complex	3.50	0.93	3.20	1.80	6.70	0.39	1.90	125.00
Co- cefovecin complex	30.85	10.63	15.58	1.69	61.40	0.14	1.28	1.08
Ni- cefovecin complex	124.95	55.95	31.20	1.26	499.90	3.80	1.60	1.16
Cu- cefovecin complex	0.07	1.00	6.80	1.18	1.85	0.06	0.90	15.58
Zn- cefovecin complex	30.85	15.58	7.76	0.93	62.40	0.14	1.85	0.93
Cd- cefovecin complex	30.85	15.58	5.11	2.67	22.59	0.39	0.73	0.94
Hg- cefovecin complex	0.07	0.24	0.28	2.10	2.95	1.40	2.30	15.63

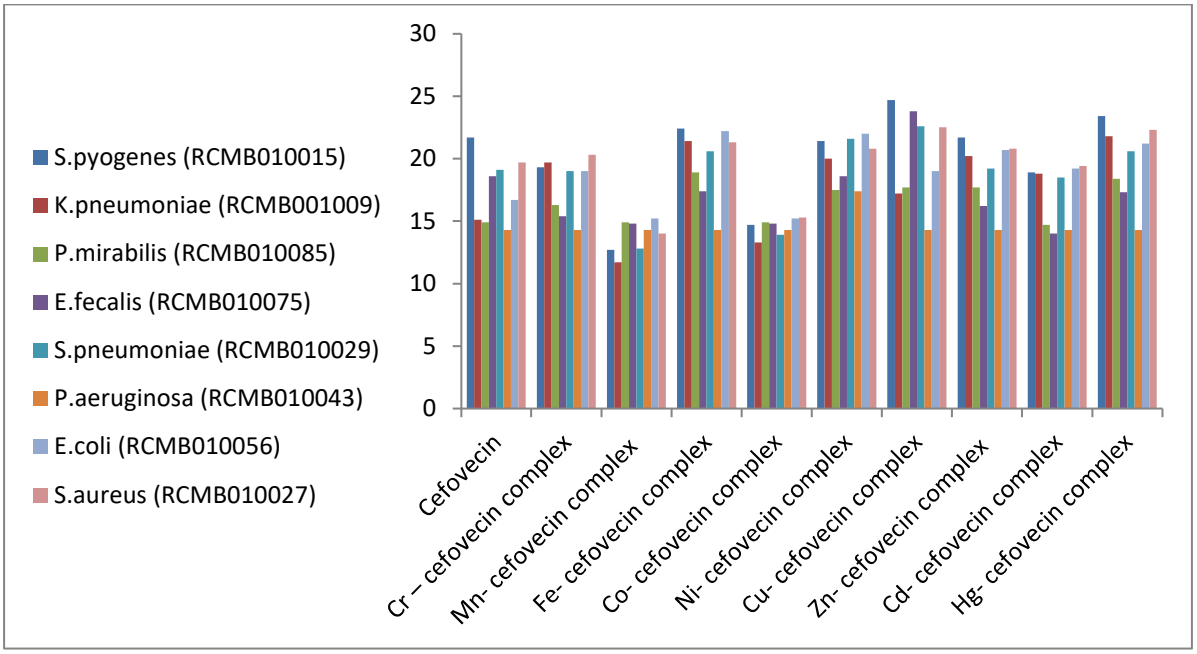

Figure 20: Antibacterial activity of cefovecin and its metal complexes against 8 different bacterial species

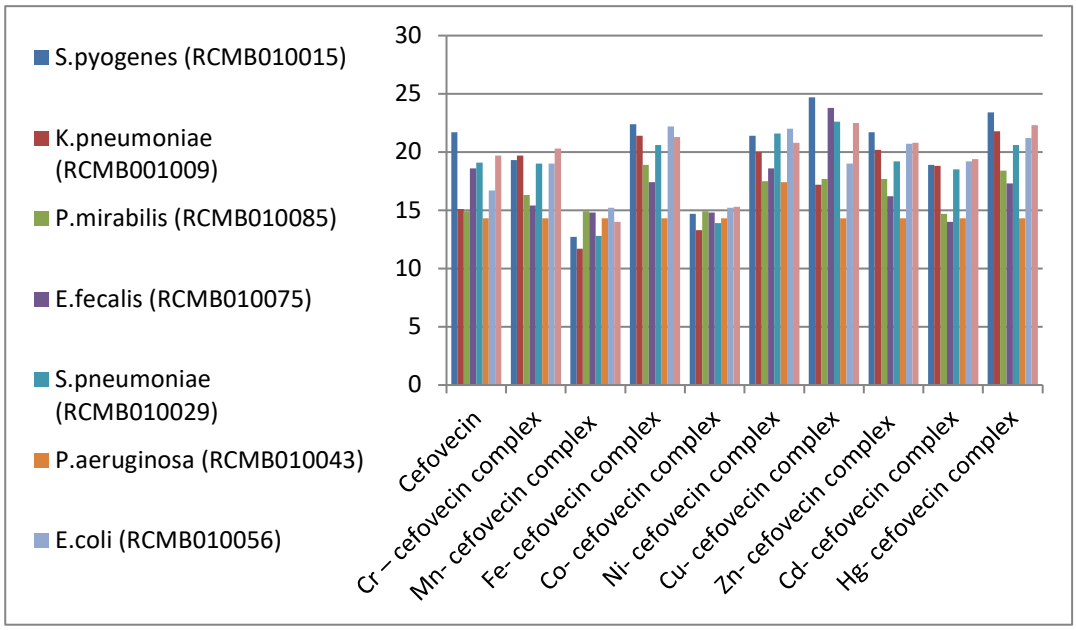

Figure 21: Antifungal activity of Cefovecin and its metal complexes against 8 fungal species

Conclusion

Nine metals Biologically active complexes of cefovecin were prepared and characterized using IR, UV-Vis, ESR, magnetic susceptibility, thermal analysis (TGA and DTA). IR data pointed that all complexes were suggested that cefovecin coordinates to the metal ions as a bidentate with stochiometries 1:1 (M: L). Electronic absorption spectra gathered with the magnetic moment values proved that all cefovecin complexes have octahedral geometry. The calculated room temperature powdered ESR data of copper cefovecin complex showed anisotropic spectra. Thermal analyses (TGA and DTA) of ligands and their metal complexes were carried out to distinguish between the coordinate and hydrate solvents and to estimate the stability ranges. The thermodynamic parameters, such as activation energy (ΔE*), enthalpy of activation (ΔH*), entropy of activation (ΔS*) and Gibbs free energy (ΔG*) are calculated and discussed. Mössbauer spectroscopy, D.C conductivity measurements and Dielectric constant, A.C. conductivity are discussed. Antimicrobial activities were screened for some metal complexes of cefovecin.

References

[1]. Pfizer Animal Health. "Convenia". Pfizer. (2013).https://web.archive.org/web/ 20120411102024/ https://cdn.pfizer.com/pfizercom/products/pah_media_fact_sheet.pdf

[2]. J.E. Maddison, S.W. Page, D.B. Church, "Chapter 8: Antibacteria drugs. Cephalosporins and cephamycins". Small animal clinical pharmacology (2nd ed.). Edinburgh: Saunders/Elsevier. pp. 164–168 (2008). ISBN 9780702028588.

[3]. Antibiotic injection for canine and feline bacterial skin infections (2013), Distributed by: Zoetis Inc. Kalamazoo, MI 49007 Zoetis Services LLC. https://www2.zoetisus. com/content/_assets/docs/vmips/package-inserts/convenia_insert.pdf

[4]. D.M. Boothe, "Chapter 7: Antimicrobial drugs". In Small animal clinical pharmacology & therapeutics(2nd ed.). Elsevier Saunders (2012). ISBN 9781437723571.

[5]. S.A. Kolkaila, A.E. Ali, G.S. Elasala, Synthesis, Spectral Characterization of Azithromycin with Transition Metals and a Molecular Approach for Azithromycin with Zinc for COVID-19, Int J Cur Res Rev., 13, 23, 53-59, (2021).

[6]. A.E. Ali, G.S. Elasala, E.A. Mohamed, S.A. Kolkaila, Spectral, thermal studies and biological activity of pyrazinamide complexes, Heliyon, 5, 11, e02912, (2019).

[7]. M.S. Masoud, A.E. Ali, G.S. Elasala, S.A. Kolkaila, Synthesis, spectroscopic, biological activity and thermal characterization of ceftazidime with transition metals, Spectrochimica Acta Part A: Molecular and Biomolecular Spectroscopy, 193, 458-466, (2018).
[8]. M.S. Masoud, A.E. Ali, G.S. Elasala, S.A. Kolkaila, Spectroscopic Studies and Thermal Analysis on Cefoperazone Metal Complexes, Journal of Chemical and Pharmaceutical Research, 9, 4, 171-179, (2017).
[9]. A.E. Ali, G.S. Elasala, E.A. Mohamed, S.A. Kolkaila, Structural and thermal analysis of some imipramine complexes, Materials Today: Proceedings, 45, 3692-3698, (2021).
[10]. G. Schwarzenbach, "Complexometric Titration", Translated by H. Irving, Methuen Co., London, (1957).
[11]. A. I. Vogel, "A Text Book of Quantitative Inorganic Analysis", Longmans, London (1989).
[12]. R.H. Lee, E. Griswold, J. Kleinberg, Studies on the stepwise controlled decomposition of 2,2'-bipyridine complexes of cobalt(II) and nickel(II) chlorides, Inorg. Chem., 3, 9, 1278-1283 (1964).
[13]. B. N. Figgis, J. Lewis, "Modern Coordination Chemistry", Interscience, New York, p. 403, (1967).
[14]. H. Agwa, M. M. Aly and R. Bonaly, Isolation and characterization of two Streptomyces species produced non polyenic antifungal agents. J. Union. Arab. Biol. 7, 62-82 (2000).
[15]. J. H. Doughari Antimicrobial activity of Tamarindus indica Linn. Trop. J. Pharm. Res. 5(2), 597-603 (2006).
[16]. M. S. Masoud, A. E.Ali, M. A. Shaker and G. S. Elasala, Synthesis, computational, spectroscopic, thermal and antimicrobial activity studies on some metal-urate complexes, Spectrochim. Acta A., 90, 93-108 (2012).
[17]. M. S. Masoud, O. H. Abd El- Hamid and Z. M. Zaki, 2-Thiouracil-based cobalt (II), nickel (II) and copper (II) complexes, Trans. Met. Chem, 19, 21-24 (1994).
[18]. M. G. Abd El-Wahed, M. S. Refat and S. M. El-Megharbel, Spectroscopic, thermal and biological studies of coordination compounds of sulfasalazine drug: Mn(II), Hg(II), Cr(III), ZrO(II), VO(II) and Y(III) transition metal complexes, Bull. Mater. Sci., 32 (2), 205-214 (2009).
[19]. M. S. Masoud, E. A. Khalil, O. H. A. El. Hamid and A. A. Soayed, Effect of salinities and sodium nitrite on the ionization of 2-thiouracil and some of their substituted phenylazo compounds, The Egyptian Science Magazine 2 (2), 33-37 (2005).
[20]. M.B.H. Howlader, M.S. Islam and M. R. Karim, Synthesis of some 16-membered macrocyclic complexes of chromium(III), manganese(II), iron(III), cobalt(II), nickel(II) and copper(II) containing a tetraoxooctaazacyclohexadecane ligand, Indian J. Chem, 39 A, 407-409 (2000).
[21]. A. Sreekanth, M. Joseph, H. K. Fun and M. R. P. Kurup, Formation of manganese (II) complexes of substituted thiosemicarbazones derived from 2-benzoylpyridine: Structural and spectroscopic studies. Polyhedron 25(6), 1408 – 1414 (2006).
[22]. E. K. Barefield, D. H. Busch and S. M. Nelson, Iron, cobalt, and nickel complexes having anomalous magnetic moments, Quart. Rev, 22 (4), 457-498 (1968).
[23]. D. W. Barnum, Electronic absorption spectra of acetylacetonato complexes-II: Hückel LCAO-MO calculations for complexes with trivalent transition metal ions, J. Inorg. Nucl. Chem, 22 (3-4), 183-191 (1961); CA. 57, 6751 c (1962).
[24]. N. L. Allinger, J. C. Tai and M. A. Miller, Organic quantum chemistry. XIII. The electronic spectra of the α-Halo ketones, J. Am. Chem. Soc, 88(19), 4495-4499 (1966).
[25]. A.B.P. Lever and D. Ogden, Haloacetate complexes of cobalt(II), nickel(II), and copper(II), and the question of band assignments in the electronic spectra of six-co-ordinate cobalt(II) complexes, J. Chem. Soc. A, 2041-2048 (1967).
[26]. A. B. P. Lever, "Inorganic Electronic Spectroscopy", Elsevier publish Co, Amster dam, 1968.
[27]. R. L. Carlin and M. J. Baker, The nitrate group as a ligand in some amine oxide complexes, J. Chem. Soc, 5008-5014 (1964).
[28]. J. E. Wertz and J. R. Bolton, Electron spin resonance elementary theory and practical applications, McGraw-Hill, Inc., New York, Library of Congress Catalog Number 77-154239, pp. 449 (1972).

[29]. H.A. Kuska, M.T. Rogers and R.E. Drullinger, Effect of Substituents on the Anisotropic ESR Parameters in Copper Acetylacetonates, J. Phys. Chem. 71, 109-114 (1967).
[30]. M. S. Masoud and M. Y. Abd El-Kaway, Infrared and Electron Spin Resonance Spectral Studies of Some Copper Purine and Pyrimidine Complexes, Spectrochim. Acta, 102A, 175-185 (2013).
[31]. V. A. Sawant, B. A. Yamgar, S. K. Sawant and S. S. Chavan, Synthesis, structural characterization, thermal and electrochemical studies of mixed ligand Cu(II) complexes containing 2-phenyl-3-(benzylamino)-1,2 dihydroquinazoline-4-(3H)-one and bidentate N-donor ligands, Spectrochim. Acta A, 74 (5), 1100-1106 (2009).
[32]. D.P. Riley, P.H. Merrell, J.A. Stone, D.H. Busch, Five- and six-coordinate complexes of iron (II) and (III) with a macrocyclic tetradentate ligand, Inorg. Chem. 14, 3, 490 –494 (1975).
[33]. H.R. Oswold and E. Dubler, "Thermal Analysis", Edited by H.G. Wiedemanm, Volume 2, Switzerland (1972).
[34]. B. Tareev, "Physics of Dielectric Materials" Mir Publishers, Moscow (1979).
[35]. P.J. Harrop, "Dielectrics", B. Worths (ed.), London (1972).